JOURNAL OF MATERIALS SCIENCE 26 (1991) 1093–1100

Oxidation behaviour and protection of carbon/carbon composites

S. M. GEE, J. A. LITTLE
Department of Materials Science and Metallurgy, University of Cambridge, Pembroke Street, Cambridge CB2 3QZ, UK

The oxidation behaviour of carbon/carbon composite materials and graphite (in cube form), in flowing air, has been studied in the temperature range 500 to 1100 °C. Gasification for unprotected samples occurred at temperatures around 500 °C. SiC coatings offered only limited protection below their intrinsic protection range due to the diffusion of oxygen along microcracks. Diffusional control was more significant for thicker coatings. However, the use of boron oxide applied on an underlayer of SiC, gave good protection for extended periods at temperatures up to 1000 °C, due to microcrack sealing. The use of borate coatings, both with and without an SiC underlayer, was limited by the volatility of the borate.

1. Introduction

Carbon fibre-reinforced carbon matrix composites (C/C composites) are potentially useful materials in applications requiring strength and toughness, at high temperatures combined with low weight [1]. Potential uses range from those in aircraft, hypersonic aerospace vehicles and the automotive industry, to biomedical and refractory applications. These composites retain their strength, modulus and mechanical properties to temperatures higher than those tolerated by other materials [2, 3].

Strong covalent bonding gives a low carbon atom diffusivity which, combined with the highly anisotropic graphite crystal structure, suggests exceptional creep resistance for graphitic carbons [4]. However, the rapid reaction of carbon with oxygen at temperatures as low as 500 °C causes rapid degradation of the composite [5] and thus effective oxidation protection for C/C composites at temperatures of 1000 °C and above must be developed.

Both inhibitors, such as phosphorus and the halogens incorporated into the graphite matrix [6, 7] and oxygen diffusion barriers [4, 5, 8, 9] have been investigated and this paper reports the role of an SiC chemical vapour deposited (CVD) barrier both with and without boron oxide on both graphite and a C/C composite. Additives such as boron oxide can form liquid glassy phases which can flow at temperature thus sealing cracks in the applied coating [2], cracks due to the differing thermal expansion coefficients between the composite and SiC.

2. Experimental procedure

The C/C composite materials (K-Karb) used in this study were made from rayon-based carbon fibres and a carbonized phenolic resin impregnated matrix, in a two-dimensional fibre mat lay-up (Fig. 1a and b). The graphite was a high density isotropic grade (Poco EDM3). Both were supplied by BP Sunbury Laboratories, in block form. Five samples of C/C composite in approximately cube form, side ~ 10 mm, were supplied with CVD SiC coatings of varying thicknesses. One graphite sample, of similar dimensions, was also SiC coated. B_2O_3 was prepared as a paste, in glycerol, and applied to specimens using a wooden spatula. The coated sample was then fired at 500 °C to consolidate the coating. Bulk densities were calculated from the total mass and volume of the block samples. All dimensions were measured using Vernier calipers and masses measured on a microbalance accurate to $\pm 0.000\,01$ g. The densities were calculated as 1.9 g cm^{-2} (graphite) and 1.6 g cm^{-2} (C/C composite).

Measurements of the oxidation kinetics of all samples were carried out in a vertically mounted furnace, in flowing air (80% N_2, 20% O_2, flow rate ~ 6 ml min^{-1}), between 500 and 1200 °C. The specimen was held in a platinum wire cage suspended on steel wire links from the mass balance. Mass changes of the specimens were measured as functions of time using a Stanton Redcroft mass balance (sensitivity ± 1 mg) and a Stanton Redcroft chart-pen recorder. The temperature of the furnace was controlled using a Eurotherm regulator and ramped by hand.

All kinetic data were obtained by ramping the furnace between temperatures and isothermally holding the specimen to allow sufficient data to be collected. At low temperatures, ramping rates of ~ 20 °C min^{-1} were achieved, but above ~ 1000 °C the rates were significantly less. Specimens were allowed to cool in air and were characterized using reflected light and scanning electron microscopy.

3. Results and discussion

3.1. Oxidation behaviour of uncoated C/C composites and graphite

Fig. 2 shows oxidation rates, as a function of temperature, for C/C composite and graphite samples in

0022–2461/91 $03.00 + .12 © *1991 Chapman and Hall Ltd.*

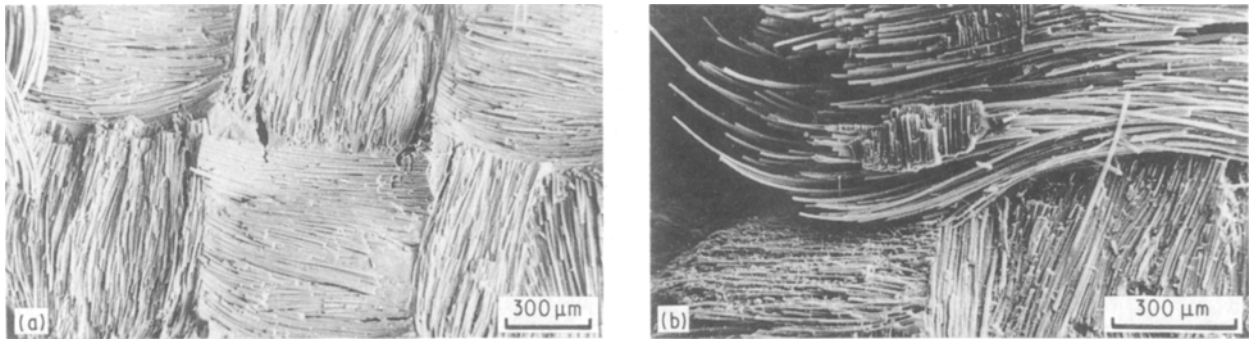

Figure 1 SEM micrographs of 2D fibre mat lay-up.

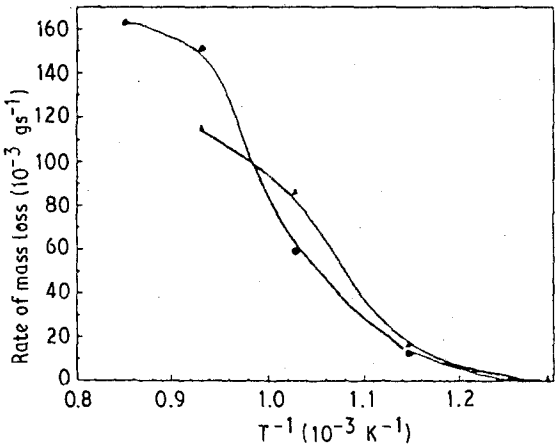

Figure 2 Oxidation rates for carbon–carbon composite and graphite samples. (●) C/C composite (▲) graphite.

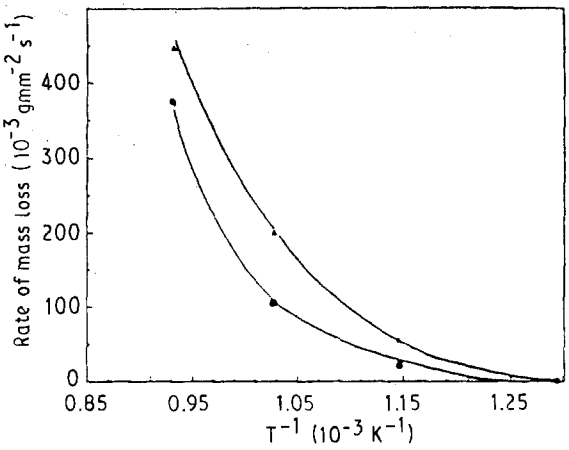

Figure 3 Oxidation rates plotted as a function of decreasing geometrical area. (●) C/C composite (▲) graphite.

flowing air. At temperatures up to ~ 700 °C both samples showed a marked increase in oxidation rate with temperature. However, above ~ 700 °C this increase was notably reduced, with the curves starting to flatten out. On removal from the furnace the samples were seen to have decreased their lateral dimensions by up to 50% and it is suggested that the decrease in geometric area of the samples caused this apparent lowering of the oxidation rate. However, due to the presence of porosity, the effective surface area over which the reaction can occur is possibly 10 to 100 times higher than the geometric area [10]. The oxidation threshold for both the C/C composite and graphite was ~ 525 °C.

Fig. 3 shows oxidation rates per unit of geometrical area as a function of temperature, for the same experiment. The average geometrical surface area of the specimen at each temperature was calculated by finding the surface areas at the start and finish of the isothermal period. Assuming cube geometry, the mass of a sample m is given by

$$m = \frac{S^{3/2}D}{6^{3/2}} \quad (1)$$

where D is the density and S is the geometric surface area. For a mass change of δm, the new surface area is given by

$$S = \frac{6(m - \delta m)^{2/3}}{D^{2/3}} \quad (2)$$

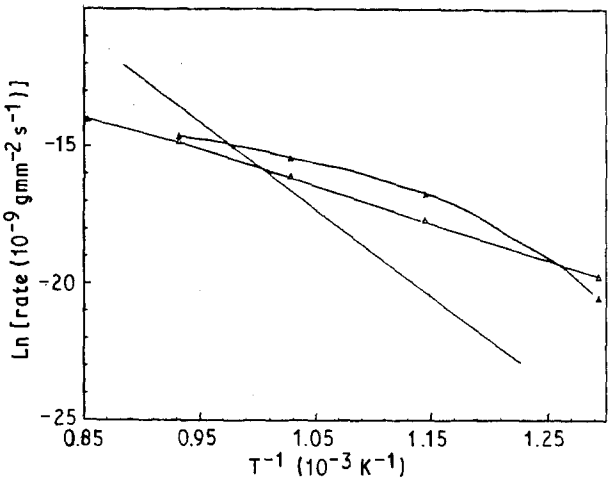

Figure 4 Arrhenius plots for the oxidation of carbon–carbon composite and graphite samples. (●) C/C composite (▲) graphite. Straight line shows Arrhenius plot for single crystal carbon [10].

Knowing the mass of the sample at the start of each isothermal period and the loss in mass during that period, Equations 1 and 2 can be used to calculate the required area. This simple treatment does eliminate the apparent drop-off in oxidation rate at high temperature. It is noted that care needs to be taken when oxidation rates are quoted per unit surface area. For specimens that undergo gross reductions in surface area, the above treatment may be useful. Using sheet materials, however, can effectively eliminate this effect. In the case of coated specimens, the dimensions of the

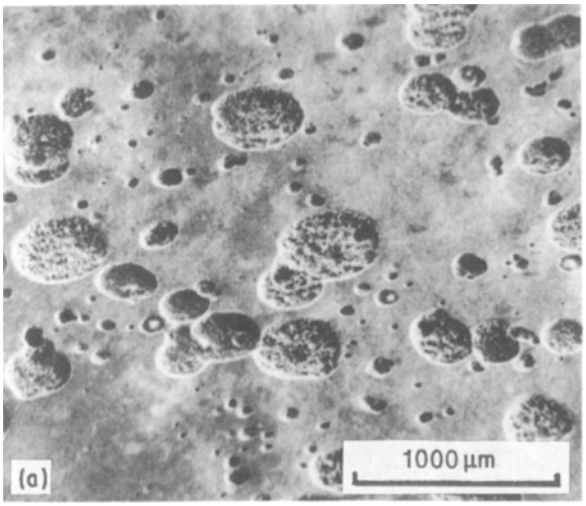

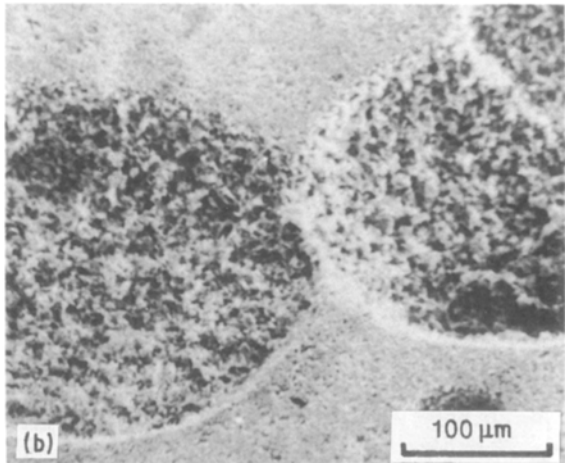

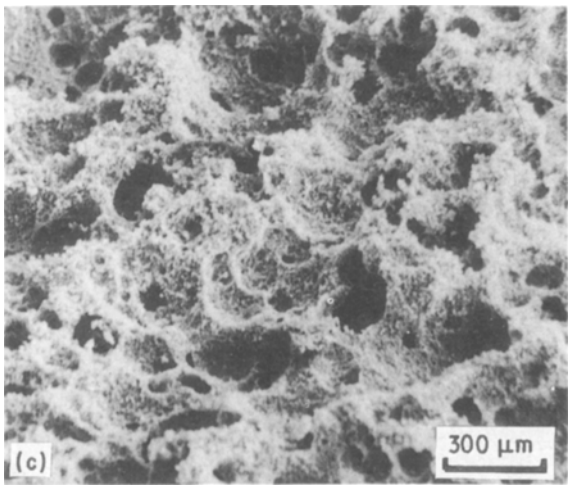

Figure 5 SEM micrographs showing the development of the oxidation morphology on graphite.

samples do not change significantly and the geometrical surface area is quoted.

Fig. 4 shows Arrhenius plots for the oxidation of the C/C composite and graphite in flowing air, for rates measured per unit of geometrical surface area. These show apparent activation energies of $\sim 110\,kJ\,mol^{-1}$ for the C/C and a similar value for the graphite at high temperatures with a somewhat higher value at low temperatures. Ubbelhode and Lewis [11] have discussed the nature of graphite oxidation in terms of a first step and succession steps mechanism. For graphite oxidation in air (1 atm), the low-temperature rate-limiting step was likely to be the desorption of "surface oxide" from the carbon network, to give CO and CO_2 (succession steps). At higher temperatures the release of the oxidation products, leaving defects in the carbon network, became easier. The rate was then probably controlled by oxygen diffusion into pores and adsorption at active sites (first step). This led to a lowering of the activation energy as the temperature was increased. It is well known that the kinetics of carbon gasification are affected by impurities, the concentration of active sites, degree of crystallinity, network structure and the diffusion of gases to active sites [6, 7]. Thus direct comparisons of the values of activation energies with previous work are difficult. However, the values for graphite were similar to those given by other workers (100 to $150\,kJ\,mol^{-1}$).

Fig. 4 also shows the temperature dependence of oxidation rate of single-crystal carbon, based upon the virtual maximum rate of surface reaction [10] and shows that under the given conditions, C/C oxidation was controlled by the surface reaction of oxygen with active sites on the composite surface. Reaction rates for the uncoated C/C were higher, by as much as two orders of magnitude, than those for single-crystal carbon. This suggests that the effective area over which oxidation could occur was up to 100 times greater than the projected area. This is consistent with the high porosity of the C/C composite.

Oxidation of the graphite appeared to occur at specific active sites (Fig. 5a), leading to pitting

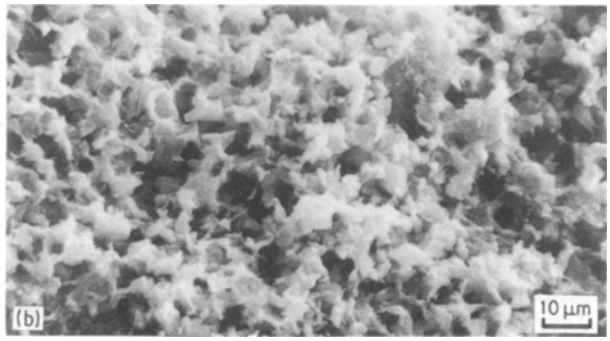

Figure 6 High magnification SEM image of the surface of oxidized graphite.

(Fig. 5b) and, after prolonged exposure at high temperatures (up to 900 °C), severe degradation and porosity at the surface (Fig. 5c). The spherical nature of the reaction sites indicated that the graphite oxidized isotropically. Oxidation proceeded preferentially between graphite flakes, leaving a much more "open" structure to the pits (Fig. 6a) than the surrounding surfaces (Fig. 6b). It has been noted that amorphous carbons, because of the higher incidence of reactive edge sites, tend to be more susceptible to gasification than crystalline graphite [2]. This may account for the observed microstructures. Prior to oxidation, the C/C composite surface was very porous. Oxidation of the matrix and fibres occurred simultaneously, with oxygen penetration into the material. After prolonged exposure at high temperatures (up to 900 °C), this resulted in severe excavation of the carbonaceous matrix from between the fibre bundles (Fig. 7a), along with degradation of the fibres themselves (Figs 7b and 8a). Pitting could be seen on remaining particles of matrix (Fig. 8b and c), in furrows left by fibres, oxidized away.

3.2. Oxidation behaviour of SiC coated C/C composites and graphite

Any coating used to protect the composite from oxidation must prevent the inward diffusion of oxygen, and have a low volatility, to prevent erosion occurring in fast-flowing gas streams. Internally, the coating must have good adherence to the substrate, with little penetration, and must be effective in preventing the outward diffusion of carbon, which could lead to the reduction of the external oxide. Finally, all interfaces must exhibit both chemical and mechanical compatibility, the latter being an overriding issue in the choice of suitable coatings.

C/C composites have lower thermal expansion coefficients, in the fibre layers, than any symmetric crystalline ceramics. Because deposition by CVD occurs at high temperature, cooling the composite inevitably leads to microcracking in the coating. Optical studies, prior to oxidation, revealed the presence of microcracks in the SiC coatings on the composite (Fig. 9). These occur on cooling from the necessarily high SiC deposition temperature, as a result of thermal expansion mismatches [4]. Oxidation results from oxygen transport along the microcracks to the underlying C/C.

Fig. 10 shows oxidation rates, as a function of temperature, for two SiC-coated C/C composites in flowing air, quoted per unit of initial geometric surface area. Reaction rates for the two coatings, of thicknesses 98 and 17 μm, were very similar for temperatures up to ~ 700 °C. However, between ~ 700 and ~ 1000 °C the rates of oxidation showed significant deviation. At ~ 950 °C the rate for the 17 μm coating was approximately four times that of the 98 μm coating. The rate dropped to zero at ~ 1050 °C (for 17 μm) and ~ 1100 °C (for 98 μm). This was a consequence of all oxidizable material having been removed from within the sample, leaving a hollow SiC shell. The oxidation threshold for both samples was ~ 600 °C.

The rate-limiting steps for C/C oxidation in the presence of a protective coating has been discussed by considering the concept of virtual maximum rate [10]. The rate limiting step is the one with the lowest virtual maximum rate. In considering diffusion through pores and cracks, the effective diffusion coefficient (D_c) is related to both the bulk (D_b) and Knudsen (D_k) diffusivities by the following relation [10]

$$(D_c)^{-1} = (D_b)^{-1} + (D_k)^{-1} \quad (3)$$

where

$$D_k = \frac{4(8RT)^{1/2}r}{3(\pi M)^{1/2}2} \quad (4)$$

r is the pore radius and M is the molecular weight of the diffusing species. The oxygen transport rate (J), at the base of the crack, can be calculated using Fick's first law

$$J = -D_c dC/\delta \quad (5)$$

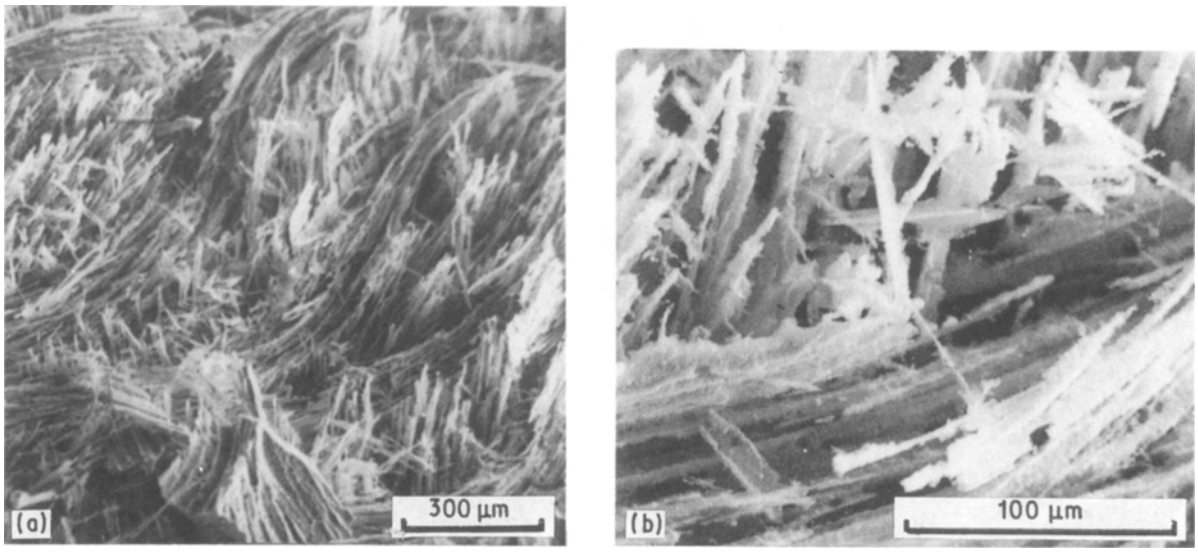

Figure 7 SEM micrograph of the oxidized carbon–carbon composite.

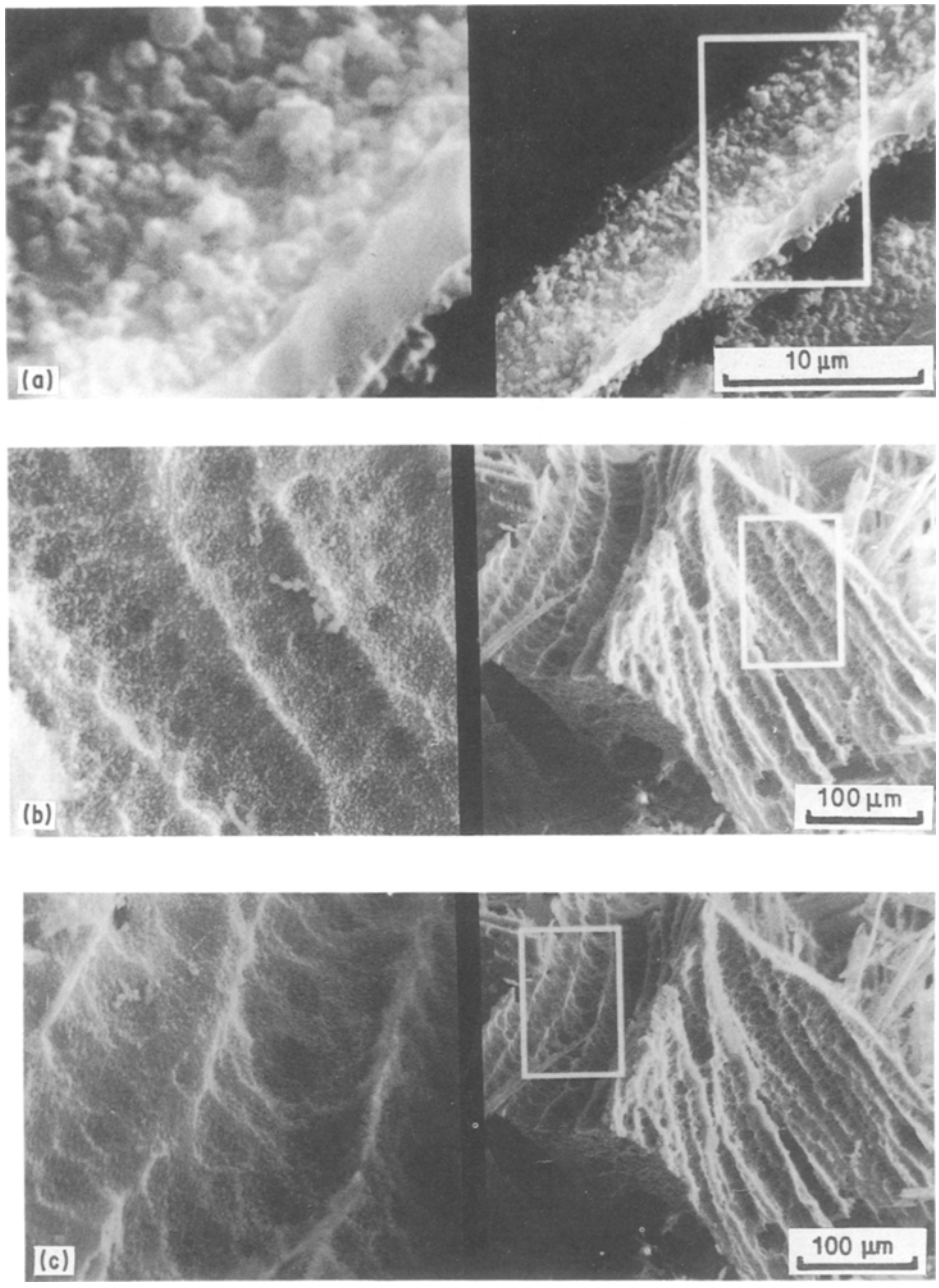

Figure 8 High magnification micrographs of oxidized carbon–carbon composite (a) degradation of carbonaceous matrix from between the fibre bundles (b) pitting of the matrix (c) furrows in matrix left by oxidized fibres.

where dC is the concentration gradient and δ is the depth of the crack. It should be noted that, for pores, the effective gas diffusivity is lower than the bulk diffusivity, due to gas molecules colliding with the pore walls. In cracks, collisions can only occur across the width. Thus a crack, with the same width as a pore, will have correspondingly higher effective and Knudsen diffusivities. Equation 4 can still, however, be used to calculate a lower bound value for D_k. Equation 5 gives a rate based on the cross-sectional area of the crack. To calculate an average rate, the expression needs to be multiplied by the fractional area of cracks in the coating.

Fig. 11 shows Arrhenius plots for the oxidation of SiC-coated C/C composites in flowing air. Below $\sim 850\,^{\circ}C$, both showed apparent activation energies of $\sim 120\,kJ\,mol^{-1}$, rates being controlled by the reaction of oxygen with reactive sites on the composite surface. The onset of oxygen diffusion control (along cracks), occurred at $\sim 890\,^{\circ}C$ for the 17 μm coating and $\sim 790\,^{\circ}C$ for the 98 μm coating. Obviously, for a greater coating depth (and hence crack depth), rate limitations due to oxygen diffusion along cracks, will set in earlier as higher temperatures are reached. Equation 5 predicts a six-fold difference in oxygen diffusion rates between the 17 and 98 μm coatings, assuming D_c and dC are the same in both cases. At 950 °C, oxidation rates differed by a factor of 4. Thus there is good agreement between predicted and observed values and indeed the slightly smaller observed ratio may be the result of a smaller density of microcracks in the thinner coating.

Oxidation of both the fibres and matrix occurred simultaneously within the samples, leaving a porous "skeleton" of the original structure (Fig. 12a) on the underside of the SiC coating (Fig. 12b). The original

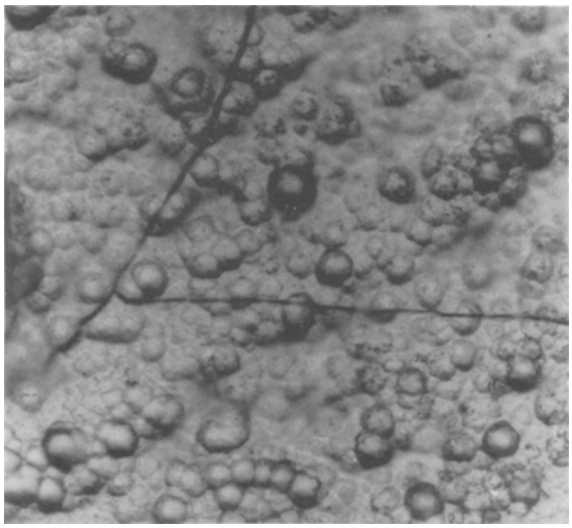

Figure 9 Optimal micrograph showing the cracked silicon carbide coating.

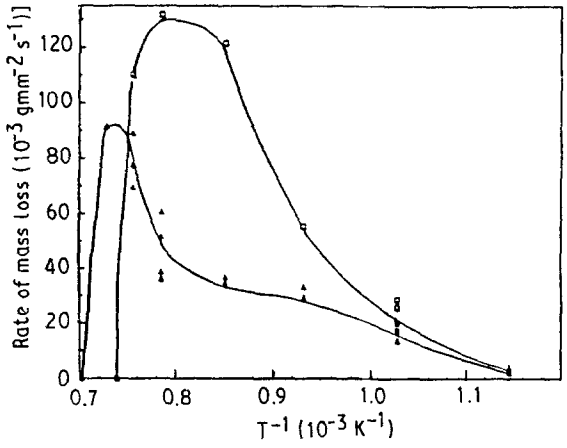

Figure 10 Oxidation rates for two silicon carbide coated carbon–carbon composites of thicknesses 98 and 17 μm. (▲) 98 micron (□) 17 micron.

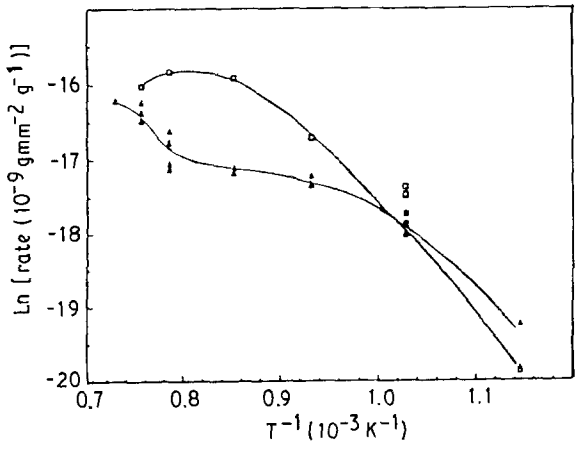

Figure 11 Arrhenius plots for the oxidation of silicon-carbide coated carbon–carbon composites in flowing air. (▲) 98 micron (□) 17 micron.

fibre mat lay-up was still clearly visible. Oxidation appeared to lead to the propagation of longitudinal channels along the fibre axes, both parallel and perpendicular to the SiC coating (Fig. 12c). Evidence of extensive reaction on the inner walls of these channels was observed (Fig. 12d). It is suggested that facile oxygen diffusion along such channels, allowed a rapid excavation of material. In all cases, the temperatures were insufficient to cause SiO_2 formation, to give crack filling. Thus the coatings were operating below their intrinsic protection range.

The influence of the microcracking of the SiC can be seen in Fig. 13 which shows the oxidation rates and Arrhenius plot for SiC-coated graphite (thickness 70.6 μm). Comparison with Fig. 3 shows the dramatic reduction in the oxidation rate resulting from coating with SiC. Consequently, the oxidation threshold was increased to ~ 600 °C.

Optical examination, prior to oxidation, failed to reveal the presence of any microcracks in the SiC coating. This is consistent with the graphite and SiC having a low thermal expansion mismatch [4]. Examination of the specimen on removal from the furnace, suggested that oxidation was initiated at the corners and edges of the sample. It is suggested that the adherence of the SiC coating at these sites was poorer than on the cube faces and that local mismatches caused some microcracking in these regions.

The Arrhenius plot shows apparent activation energies in the range 30 to 150 kJ mol^{-1}.

3.3. Oxidation behaviour of boron oxide-coated C/C composites

As the problem of microcracking occurs in any applied SiC layers on a C/C composite, boron and boron compounds are often included in the composite to form borate glasses which can flow to give crack sealing up to 1500 °C. The effect of applying a boric acid paste alone to the composite can be seen in Fig. 14 which shows oxidation rates as a function of temperature, in flowing air. The B_2O_3 coating offered excellent oxidation protection up to a temperature of ~ 650 °C. Above this temperature, the rate accelerated dramatically, increasing non-linearly with time throughout the isothermal period. This was a result of the volatilization of the coating, leaving the underlying C/C exposed.

Fig. 15 shows an Arrhenius plot for the same experiment. Apparent activation energies were in the range 0 to 250 kJ mol^{-1}. Oxidation was surface rate controlled and limited by the fraction of exposed substrate. The dramatic increase in the activation energy at higher temperatures, was in direct contrast to the behaviour of the uncoated C/C (Fig. 4). B_2O_3 diffusion into the porous structure of the composite may account for this inhibition of the reaction of the exposed C/C at higher temperatures.

Composite samples with a 64 μm SiC coating plus B_2O_3 showed little mass change with time up to 1000 °C (Fig. 16). The sample showed a very gradual mass loss with increasing time, due to volatilisation of the B_2O_3 coating. Cooling the sample in air, to room temperature, and reheating to 900 °C, did not increase the rate of oxidation. Hence microcracks initially present in the coating, as well as those introduced as a result of cooling the sample to room temperature,

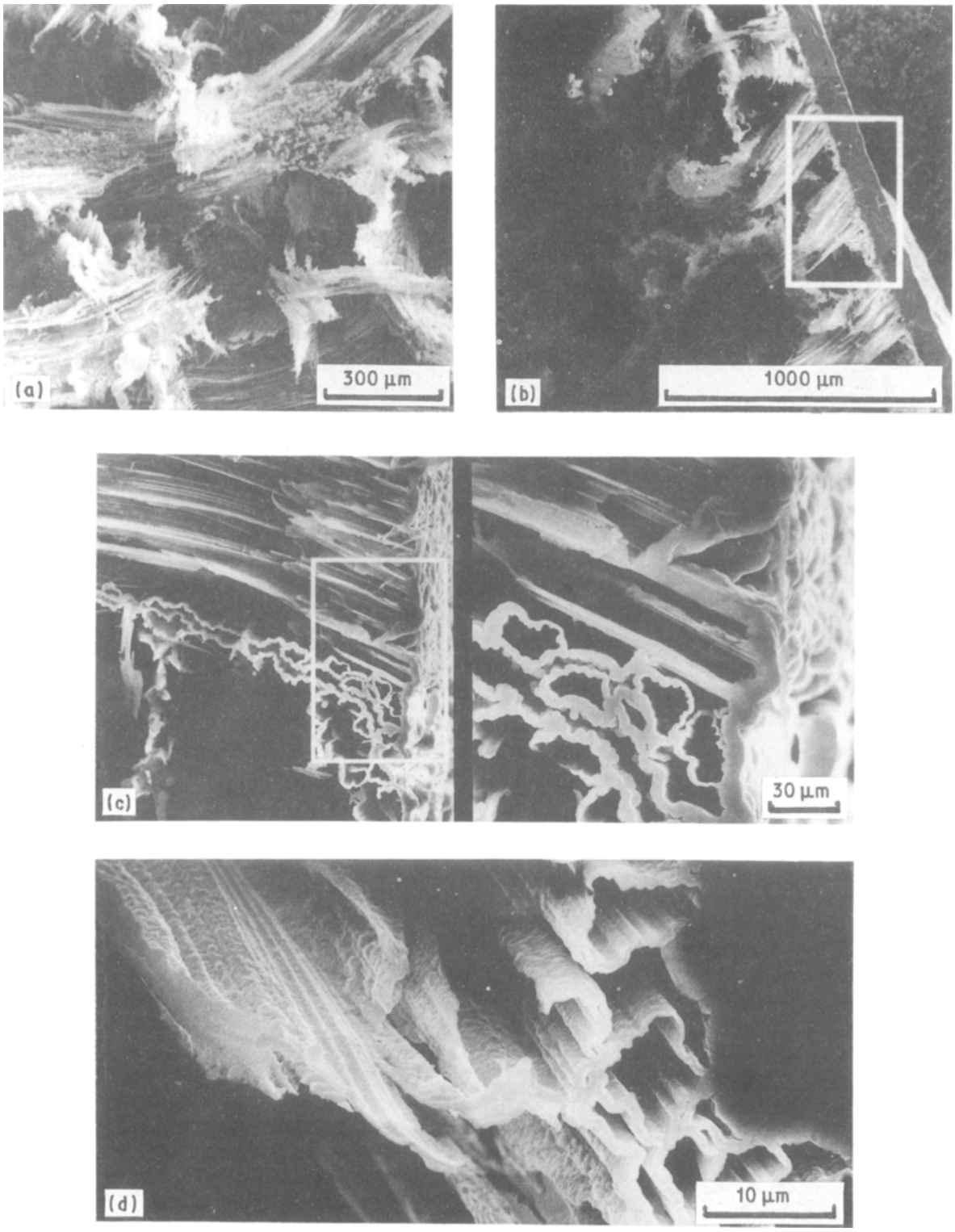

Figure 12 (a) Oxidation of both fibres and matrix in coated composite (b) remaining composite on underside of coating (c) longitudinal channels in the composite after oxidation (d) reaction of inside walls of channels after oxidation.

were effectively sealed by the borate glass. Comparison with Fig. 10 shows the extent of the oxidation protection afforded by the duplex coating.

4. Conclusions

Carbon/carbon composite materials and graphite, in cube form, begin to oxidize in flowing air, at ~ 500 °C.

For graphite, oxidation rates at low temperatures are surface reaction rate controlled, while at higher temperatures rates are limited by the desorption of oxidation products from the surface. The reaction occurs isotropically and appears to be initiated at selected "active" sites.

At all temperatures up to 900 °C, C/C composite oxidation is surface reaction rate controlled under the experimental conditions given. SiC coatings offer protection to C/C composites for only limited periods below the intrinsic protection range, due to the presence of microcracks. At low temperatures, oxidation is surface reaction rate controlled while oxygen diffusion along microcracks becomes important as higher

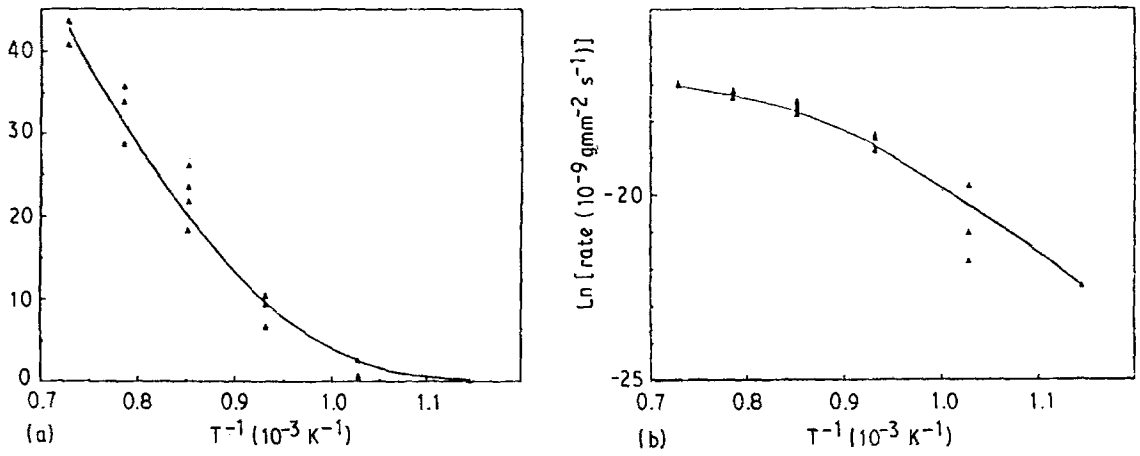

Figure 13 Oxidation rate and Arrhenius plot for the silicon carbide coated carbon–carbon composite.

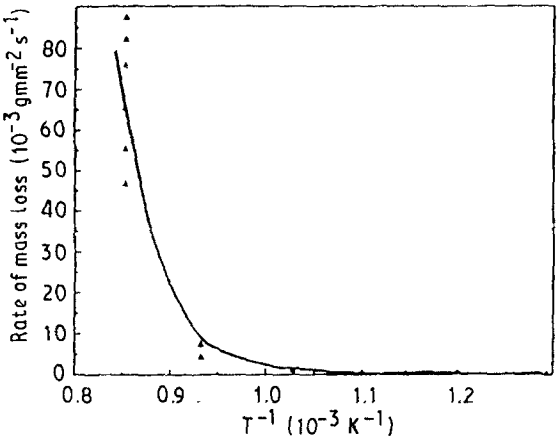

Figure 14 Oxidation rate of composite coated with boric oxide.

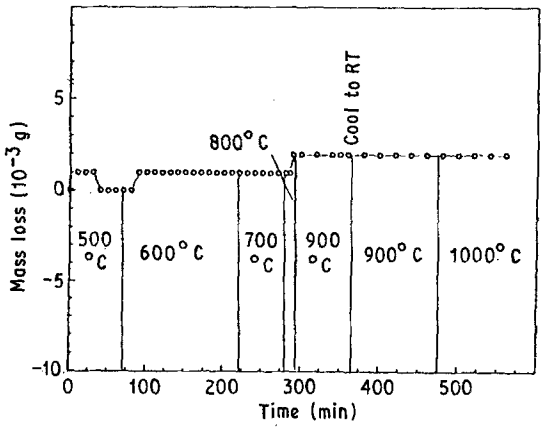

Figure 16 Oxidation rates of carbon–carbon composite coated with 64 μm of silicon carbide and a layer of boric oxide.

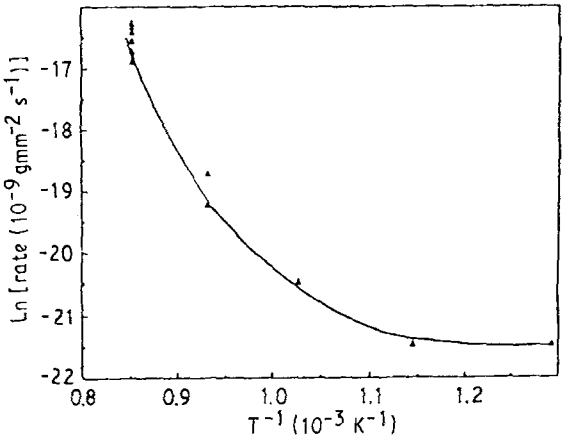

Figure 15 Arrhenius plot for oxidation of boric oxide coated composite (from Fig. 14).

temperatures are reached. The onset for diffusion control occurs at lower temperatures for thicker coatings.

Boron oxide, applied directly to the C/C composite surface, offers protection up to a temperature ~ 650 °C. The fluidity of the glass above 500 °C ensures effective microcrack sealing on thermal cycling. The duplex SiC B_2O_3 coating offers excellent protection up to ~ 1000 °C.

References

1. J. D. BUCKLEY, *Amer. Ceram. Soc. Bull.* **67** (1988) 364.
2. D. W. McKEE, *Carbon* **24** (1987) 551.
3. E. FITZER and R. GADOW, *Amer. Ceram. Soc. Bull.* **65** (1986) 326.
4. J. R. STRIFE and J. E. SHEEHAN, *ibid.* **67** (1988) 369.
5. D. W. McKEE, *Carbon* **24** (1986) 737.
6. *Idem*, in "Chemistry and Physics of Carbon", Vol. 16 (Marcel Dekker, New York, 1981) p. 1.
7. I. JAWED and D. C. NAGLE, *Mater. Res. Bull.* **21** (1986) 1391.
8. P. EHRBURGER, P. BARANNE and J. LAHAYE, *Carbon* **24** (1986) 495.
9. G. SAVAGE, *Metals and Materials* September (1988) 544.
10. K. L. LUTHRA, *Carbon* **26** (1988) 217.
11. A. R. UBBELHODE and F. A. LEWIS, "Graphite and its crystal compounds" (Oxford University Press, Oxford, 1960).

Received 26 June
and accepted 1 December 1989